

# Comparison of performance of self-expanding and balloon-expandable transcatheter aortic valves



Hoda Hatoum, PhD,<sup>a,b</sup> Milad Samaee, PhD,<sup>c</sup> Janarthanan Sathananthan, MBChB, MPH,<sup>d</sup> Stephanie Sellers, MSc, PhD,<sup>d</sup> Maximilian Kuetting, PhD,<sup>e</sup> Scott M. Lilly, MD, PhD,<sup>f</sup> Abdul R. Ihdayhid, MBBS, PhD,<sup>g</sup> Philipp Blanke, MD,<sup>h</sup> Jonathon Leipsic, MD,<sup>h</sup> Vinod H. Thourani, MD,<sup>i</sup> and Lakshmi Prasad Dasi, PhD<sup>c</sup>

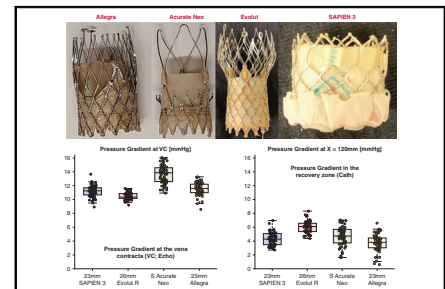
## ABSTRACT

**Objective:** To evaluate the flow dynamics of self-expanding and balloon-expandable transcatheter aortic valves pertaining to turbulence and pressure recovery. Transcatheter aortic valves are characterized by different designs that have different valve performance and outcomes.

**Methods:** Assessment of transcatheter aortic valves was performed using self-expanding devices (26-mm Evolut [Medtronic], 23-mm Allegra [New Valve Technologies], and small Acurate neo [Boston Scientific]) and a balloon-expandable device (23-mm Sapien 3 [Edwards Lifesciences]). Particle image velocimetry assessed the flow downstream. A Millar catheter was used for pressure recovery calculation. Velocity, Reynolds shear stresses, viscous shear stress, and pressure gradients were calculated.

**Results:** The maximal velocity at peak systole obtained with the Evolut R, Sapien 3, Acurate neo, and Allegra was  $2.12 \pm 0.19$  m/sec,  $2.41 \pm 0.06$  m/sec,  $2.99 \pm 0.10$  m/sec, and  $2.45 \pm 0.08$  m/sec, respectively ( $P < .001$ ). Leaflet oscillations with the flow were clear with the Evolut R and Acurate neo. The Allegra shows the minimal range of Reynolds shear stress magnitudes (up to 320 Pa), and Sapien 3 the maximal (up to 650 Pa). The Evolut had the smallest viscous shear stress magnitude range (up to 3.5 Pa), and the Sapien 3 the largest (up to 6.2 Pa). The largest pressure drop at the vena contracta occurred with the Acurate neo transcatheter aortic valve with a pressure gradient of  $13.96 \pm 1.35$  mm Hg. In the recovery zone, the smallest pressure gradient was obtained with the Allegra ( $3.32 \pm 0.94$  mm Hg).

**Conclusions:** Flow dynamics downstream of different transcatheter aortic valves vary significantly depending on the valve type, despite not having a general trend depending on whether or not valves are self-expanding or balloon-expandable. Deployment design did not have an influence on flow dynamics. (JTCVS Open 2022;10:128-39)



Comparison of self- and balloon-expandable TAV performance.

## CENTRAL MESSAGE

Flow dynamics downstream of different TAVs vary significantly depending on valve type and size, despite not having a general trend depending on whether valves are self-expanding or balloon expandable.

## PERSPECTIVE

TAVs are characterized by different designs (eg self-expanding vs balloon-expandable) that dictate different valve performance and outcomes. This study aims to evaluate the flow dynamics downstream of self-expanding and balloon TAVs pertaining to turbulence and pressure recovery. More studies are needed to correlate hemodynamic data with those observed in vivo.

From the <sup>a</sup>Department of Biomedical Engineering, and <sup>b</sup>Health Research Institute, Center of Biocomputing and Digital Health and Institute of Computing and Cybernetics, Michigan Technological University, Houghton, Mich; <sup>c</sup>Biomedical Engineering Department, Georgia Institute of Technology, Atlanta, Ga; <sup>d</sup>Center for Cardiovascular Innovation, Cardiovascular Translational Laboratory, and <sup>e</sup>Department of Radiology, St Paul's Hospital, University of British Columbia, Vancouver, British Columbia, Canada; <sup>f</sup>New Valve Technology, Hechingen, Germany; <sup>g</sup>Division of Cardiovascular Medicine, The Ohio State University Wexner Medical Center, Columbus, Ohio; <sup>h</sup>Fiona Stanley Hospital, Harry Perkins Institute of Medical Research, Perth, Western Australia, Australia; and <sup>i</sup>Department of Cardiovascular Surgery, Marcus Valve Center, Piedmont Heart Institute, Atlanta, Ga.

Drs Hatoum and Samaee contributed equally to this article as first authors.

Received for publication Nov 2, 2021; revisions received March 20, 2022; accepted for publication April 12, 2022; available ahead of print May 16, 2022.


Address for reprints: Hoda Hatoum, PhD, Department of Biomedical Engineering, Michigan Technological University, 1400 Townsend Dr, Houghton, MI 49931 (E-mail: [hhatoum@mtu.edu](mailto:hhatoum@mtu.edu)); or Janarthanan Sathananthan, MBChB, MPH, Centre for Cardiovascular Innovation, Centre for Heart Valve Innovation, Cardiovascular Translational Laboratory, St Paul's and Vancouver General Hospital, 2775 Laurel St, Vancouver, British Columbia, Canada V5Z 1M9 (E-mail: [jsathananthan@providencehealth.bc.ca](mailto:jsathananthan@providencehealth.bc.ca)); or Lakshmi Prasad Dasi, PhD, Department of Biomedical Engineering, Georgia Institute of Technology, 387 Technology Circle, Atlanta, GA 30313 (E-mail: [lakshmi.dasi@gatech.edu](mailto:lakshmi.dasi@gatech.edu)).

2666-2736

Copyright © 2022 The Author(s). Published by Elsevier Inc. on behalf of The American Association for Thoracic Surgery. This is an open access article under the CC BY-NC-ND license (<http://creativecommons.org/licenses/by-nc-nd/4.0/>). <https://doi.org/10.1016/j.xjon.2022.04.015>

**Abbreviations and Acronyms**

- PDF = probability density function
- PG = pressure gradient
- RSS = Reynolds shear stress
- TAV = transcatheter aortic valve
- VSS = viscous shear stress

 Video clip is available online.

Current commercially available transcatheter aortic valves (TAV) are either self- or balloon-expandable. During the past 2 decades, tremendous improvements in TAV designs and materials took place to optimize valve performance and maximize its benefits.<sup>1</sup> Metals were replaced (stainless steel vs cobalt chromium) to ensure stronger and more efficient anchoring, skirts were added and later modified to limit regurgitation, and valve profiles were altered to allow minimal interference with the downstream flow. Despite these improvements, the interaction of each TAV with the flow in the aortic root is associated with nonphysiological flow properties compared with flow in a native annuli.

Clinical, in vitro, and in silico studies have shown that TAV performance varies with valve type (self-expanding vs balloon-expandable),<sup>2-5</sup> the unique design of each valve within the same type group,<sup>6-8</sup> the deployment (axial and commissural),<sup>9-11</sup> and the surrounding patient-specific anatomy.<sup>12-14</sup> It is important to evaluate the flow downstream of the aortic valve because it instructs directly on the performance parameters and ultimately durability (after sufficient follow-up). The turbulence of the flow downstream of the TAV informs on the pressure drop across the valve and explains some of the reasons behind differences in pressure recovery among different valves, as identified by different measurement modalities such as echocardiography and catheterization.<sup>15</sup> The turbulence of the flow downstream of the TAV also informs on the forces that the platelets and red blood cells undergo, in the context of general blood damage such as platelet activation, thrombus formation, and hemolysis.<sup>2,16</sup>

In this study, we aim to characterize the differences in the resulting flow dynamics and pressure recovery downstream of multiple self-expanding and balloon-expandable TAVs.

**METHODS**

The hemodynamic assessment of a 26-mm Evolut (Medtronic), a 23-mm Sapien 3 (Edwards Lifesciences), a small Acurate neo (Boston Scientific) and a 23-mm Allegra (New Valve Technologies) transcatheter heart valve was performed in a left heart simulator under pulsatile physiological conditions. These sizes are equivalent in that they treat similar-sized annuli

(20-23 mm). For the study, the TAVs were implanted into a rigid test chamber described in previous publications.<sup>2,3,9,17</sup> The aortic pressures ranged from 80 to 120 mm Hg, the peak aortic pressure was set at 24 L/min, and the heart rate at 60 beats per minute. The fluid used in the experiments was a mixture of water-glycerin (60/40 by volume) with properties similar to those of blood (density of 1060 kg/m<sup>3</sup> and a kinematic viscosity of 3.5 cSt). The valves were placed in the same annulus of the same aortic root as described in previous studies.<sup>2</sup> Flow data were acquired using ultrasonic flow probes (HXL; Transonic Inc), and pressures at all the measurement locations were measured with a Millar catheter (ADInstruments Inc). The Millar catheter was inserted along the centerline of the aortic valve chamber. Recordings of the pressure at every axial location along the ascending aorta with intervals of 5 mm downstream of the valves and 1 mm inside the valves. Position 0 mm corresponds to the most upstream measurement (ventricular), and position 120 mm corresponds to the last measurement point in the measurement region of the chamber. Fifty consecutive cardiac cycles of aortic pressure, ventricular pressure, and flow rate data were recorded at a sampling rate of 100 Hz at every measurement location. The mean transvalvular pressure gradient (PG) is defined as the average of positive pressure difference between the ventricular and aortic pressure curves during forward flow. The peak PG was obtained from the instantaneous pressure waveforms. High-speed recording en-face of the valve opening, and closing was performed at a frame rate of 1000 Hz.

Particle image velocimetry experiments were performed to assess the flow downstream of each TAV. The flow was seeded with fluorescent poly (methyl methacrylate)-rhodamine B particles with average diameter of 10 μm. A laser sheet created by pulsed neodymium-doped yttrium lithium fluoride single-cavity diode pumped solid-state laser coupled with external spherical and cylindrical lenses shone on the region of interest while acquiring high-speed images of the fluorescent particles within the downstream region. Time series recordings were acquired at a temporal resolution of 500 Hz. Phase-locked recordings were acquired to calculate the resulting flow statistical parameters (Reynolds shear stress [RSS]) over 250 images. The RSS, an established metric to evaluate turbulence and any associated blood damage potential, is a statistical quantity that is used to describe a turbulent flow field.<sup>18,19</sup> The principal RSS is calculated as per Equation 1.

$$RSS = \rho \sqrt{\left(\frac{u'u' - v'v'}{2}\right)^2 + (u'v')^2} \tag{Equation 1}$$

Where ρ is the blood density and *u'* and *v'* are the instantaneous velocity fluctuations in the *x* and *y* directions, respectively.

In addition, viscous shear stress (VSS) was also computed as per Equation 2 and probability density functions (PDF) were calculated and plotted.

$$\tau = \mu \left(\frac{du}{dy} + \frac{dv}{dx}\right) \tag{Equation 2}$$

Where τ is in Pa and μ is the dynamic viscosity in Ns/m<sup>2</sup>.

**Statistics**

The results are presented as mean ± SD. Statistical analysis was performed using JMP Pro version 15.2.0 (SAS Institute Inc). All data were distributed normally, and therefore, *t* test for paired comparison between the vena contracta and recovery zone for each valve was performed along with Tukey test for unpaired comparison for vena contracta and recovery zone gradients of all valves. The instantaneous VSS over the cardiac cycle are plotted as PDFs. The PDF displays all the values (all the range) of a certain parameter distributed over a certain region of interest and gives the relative or differential likelihood (frequency) of any parameter. The area under the probability density function curve is always equal to 1 and therefore can also be considered as a normalized histogram.<sup>20</sup>

**RESULTS**

**Downstream Flow Field**

Figure 1 shows the averaged flow velocity downstream of each of the TAVs at acceleration, peak systole, and deceleration phases. The dark streaks of red and blue vorticity contours represent the shear layers corresponding to the jet boundaries and the distance between them represents the width of the jet. As the flow starts accelerating, reaching the tip of the fully open valve leaflets, it separates from the leaflet tip and travels as a free shear layer that is a region of concentrated vorticity, an indicator of flow rotation. Because the resulting shear layers and jet stability are

consequences of the interaction between flow and leaflets, it is important to visualize the opening of the valves. Videos 1 through 4 show the gradual opening of each of the valves (Evolut R, Sapien 3, Acurate neo, and Allegra, respectively). Leaflet flutters are clear with the Evolut R and Acurate neo; however, less noticeable with the Sapien 3 and the Allegra. From a different angle, Videos 5 through 8 show the flow as imaged in the experiments, highlighting the leaflet motion during the cardiac cycle.

The maximal velocity at peak systole obtained with the Evolut R, Sapien 3, Acurate neo, and Allegra was found to be  $2.12 \pm 0.19$  m/sec,  $2.41 \pm 0.06$  m/sec,

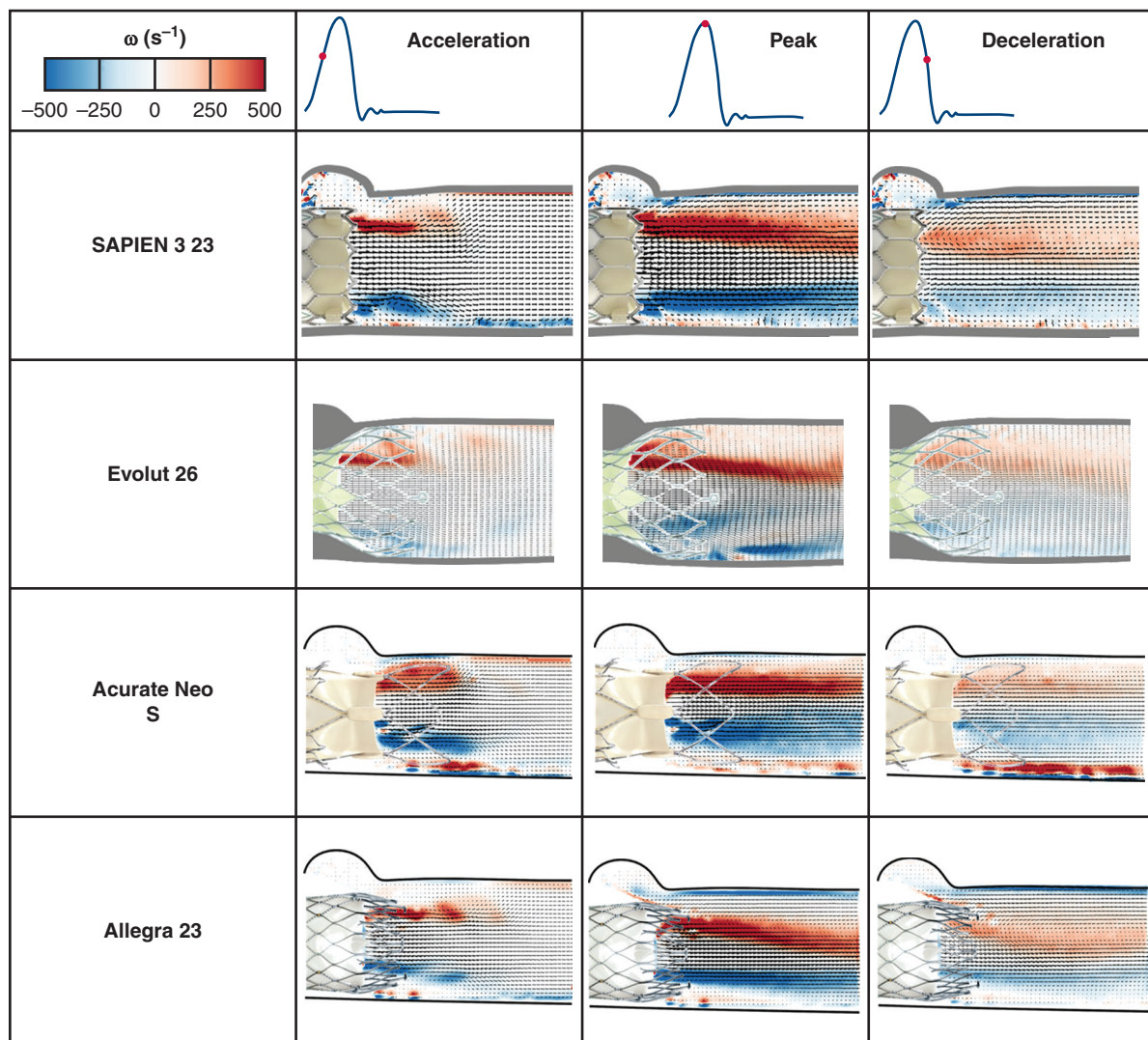
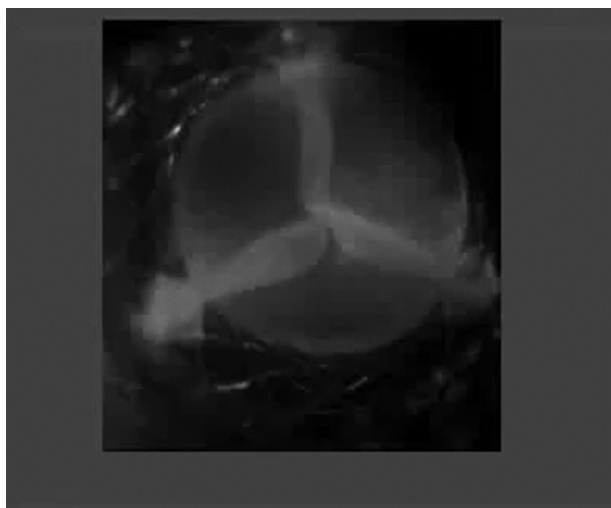


**FIGURE 1.** Phase-averaged velocity vectors and vorticity contours at different phases in the cardiac cycle. The dark streaks of red and blue vorticity contours represent the shear layers corresponding to the jet boundaries and the distance between them represents the width of the jet. The resulting shear layers and jet stability are consequences of the interaction between flow and leaflets and thus, it gives important information on the visualization of the opening of the valves and the resulting flow. The maximal velocity at peak systole obtained with the Evolut R (Medtronic), Sapien 3 (Edwards Lifesciences), Acurate neo (Boston Scientific), and Allegra (New Valve Technologies) was found to be  $2.12 \pm 0.19$  m/sec,  $2.41 \pm 0.06$  m/sec,  $2.99 \pm 0.10$  m/sec, and  $2.45 \pm 0.08$  m/sec, respectively ( $P < .001$ ).

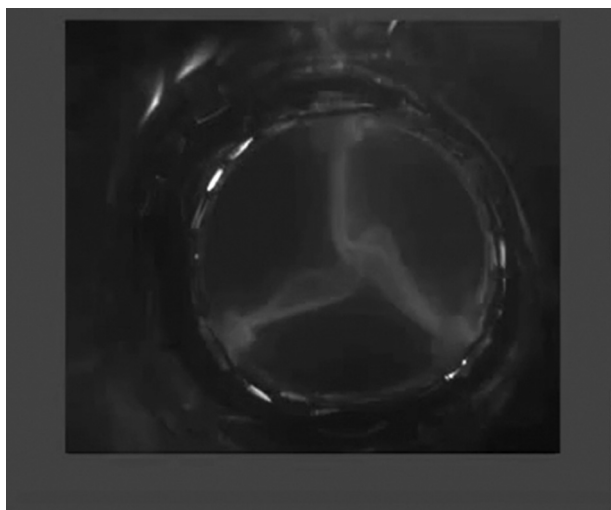


**VIDEO 1.** En-face imaging of Evolut R (Medtronic). Video available at: [https://www.jtcvs.org/article/S2666-2736\(22\)00168-1/fulltext](https://www.jtcvs.org/article/S2666-2736(22)00168-1/fulltext).

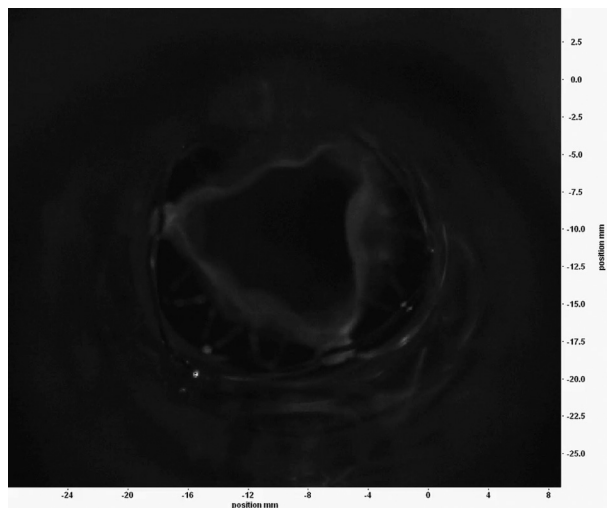
2.99 ± 0.10 m/sec, and 2.45 ± 0.08 m/sec, respectively ( $P < .001$ ). Comparing between each valve, significant differences were found except between the Sapien 3 and the Allegra ( $P = .957$ ).

**Downstream Flow Turbulence**

Figure 2 shows the principal RSS at different phases in the cardiac cycle. The maximum RSS occurs during peak systole where the flow is maximal. The dark blue patches indicate an elevated RSS magnitude, and the more prevalent elevated RSS magnitudes are, the more turbulent the flow is considered to be. The fluctuations observed in the RSS contours follow in evolution and distribution in the flow field those seen in Figure 1.

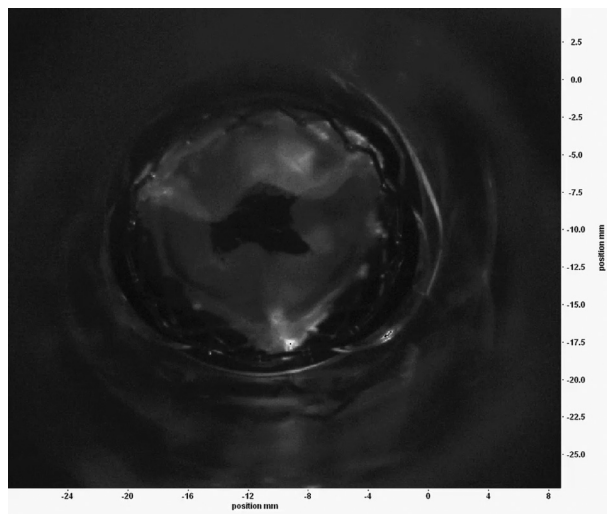


**VIDEO 2.** En-face imaging of Sapien 3 (Edwards Lifesciences). Video available at: [https://www.jtcvs.org/article/S2666-2736\(22\)00168-1/fulltext](https://www.jtcvs.org/article/S2666-2736(22)00168-1/fulltext).

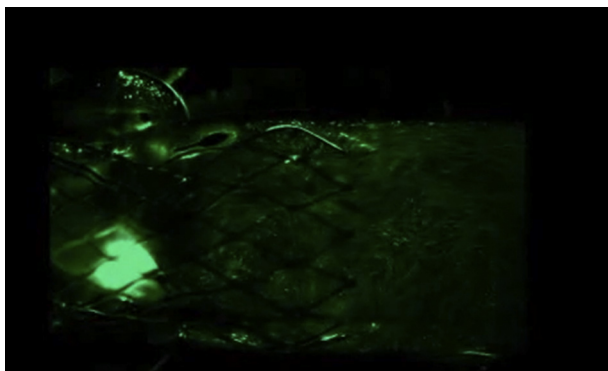


**VIDEO 3.** En-face imaging of Acurate neo (Boston Scientific). Video available at: [https://www.jtcvs.org/article/S2666-2736\(22\)00168-1/fulltext](https://www.jtcvs.org/article/S2666-2736(22)00168-1/fulltext).

To quantify the RSS distribution more accurately, Figure 3, A, shows the probability density functions of RSS for each of the TAVs at peak systole. The Acurate neo and the Evolut R present the largest distributions of RSS in all 3 phases (ie, acceleration, peak systole, and deceleration). The Allegra shows the minimal range of RSS magnitudes (up to 320 Pa), followed by the Evolut (up to 600 Pa) and then the Acurate neo and Sapien 3 (up to 650 Pa). In the literature, it was reported that a limit of 100 Pa to evaluate potential blood damage could be considered appropriate.<sup>21</sup> Any value that exceeds 100 Pa is considered elevated enough to be associated with blood damage



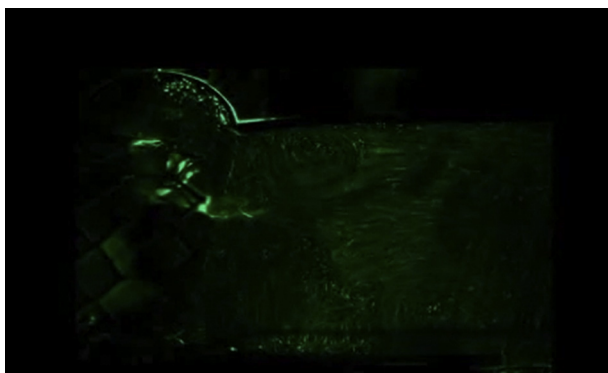
**VIDEO 4.** En-face imaging of Allegra (New Valve Technologies). Video available at: [https://www.jtcvs.org/article/S2666-2736\(22\)00168-1/fulltext](https://www.jtcvs.org/article/S2666-2736(22)00168-1/fulltext).



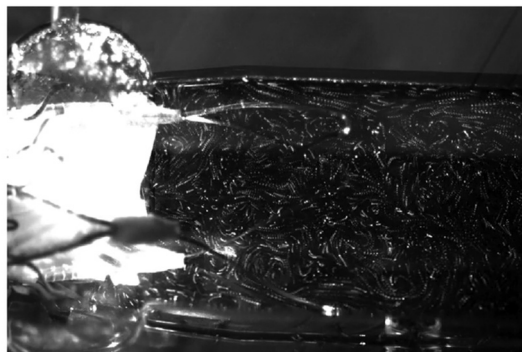
**VIDEO 5.** Raw video showing the flow downstream of the Evolut R (Medtronic). Video available at: [https://www.jtcvs.org/article/S2666-2736\(22\)00168-1/fulltext](https://www.jtcvs.org/article/S2666-2736(22)00168-1/fulltext).

potential. In **Figure 3, A**, the Sapien 3, Acurate neo, and Allegra show equal distribution of RSS <100 Pa. The Evolut shows a higher prevalence within this limit. For RSS exceeding 100 Pa, the Allegra still shows the lowest distribution. The Evolut and the Sapien 3 show equal and largest distribution up until an RSS limit of 210 Pa. When  $210 < \text{RSS} < 450$  Pa, the Acurate neo shows the largest likelihoods of development of elevated RSS. When  $\text{RSS} > 450$  Pa, the Evolut shows the highest likelihoods of elevated RSS up until 600 Pa. The Acurate neo shows more elevated likelihoods when  $\text{RSS} > 600$  Pa compared with the Sapien 3 because both these valves show such elevated magnitudes.

To evaluate the actual shear force per unit area experienced by blood elements, we calculated the instantaneous VSS for each of the valve flow fields and we plotted the probability density function of the VSS in **Figure 3, B**. All the instantaneous VSS magnitudes obtained were lower than 10 Pa, a threshold associated with potential blood damage.<sup>18</sup> The Evolut was shown to have the smallest magnitude range (up to 3.5 Pa), followed by the Allegra (up to



**VIDEO 6.** Raw Video showing the flow downstream of the Sapien 3 (Edwards Lifesciences). Video available at: [https://www.jtcvs.org/article/S2666-2736\(22\)00168-1/fulltext](https://www.jtcvs.org/article/S2666-2736(22)00168-1/fulltext).



**VIDEO 7.** Raw video showing the flow downstream of the Acurate neo (Boston Scientific). Video available at: [https://www.jtcvs.org/article/S2666-2736\(22\)00168-1/fulltext](https://www.jtcvs.org/article/S2666-2736(22)00168-1/fulltext).

4.8 Pa), followed by the Acurate neo (up to 5.5 Pa) and then the Sapien 3 (up to 6.2 Pa).

### Pressure Recovery

The importance of accounting for pressure recovery is that it permits identification of the true PG across the TAV and accordingly a more accurate assessment of performance. **Figure 4** shows the variations of PGs along selected locations in the aortic root with the 4 different valves and **Figure 5** shows the variations of the corresponding standard deviations. A box-and-whisker plot is provided for the instantaneous measurements in **Figure E1**. The results are plotted from the ventricular side upstream of each valve to the downstream side up until the end of the aortic testing chamber (at 120 mm). As the flow crosses the valve, the PG decreases from the ventricular side to the aortic 1 until it reaches a minimum at the vena contracta (where the jet is



**VIDEO 8.** Raw video showing the flow downstream of the Allegra (New Valve Technologies). Video available at: [https://www.jtcvs.org/article/S2666-2736\(22\)00168-1/fulltext](https://www.jtcvs.org/article/S2666-2736(22)00168-1/fulltext).

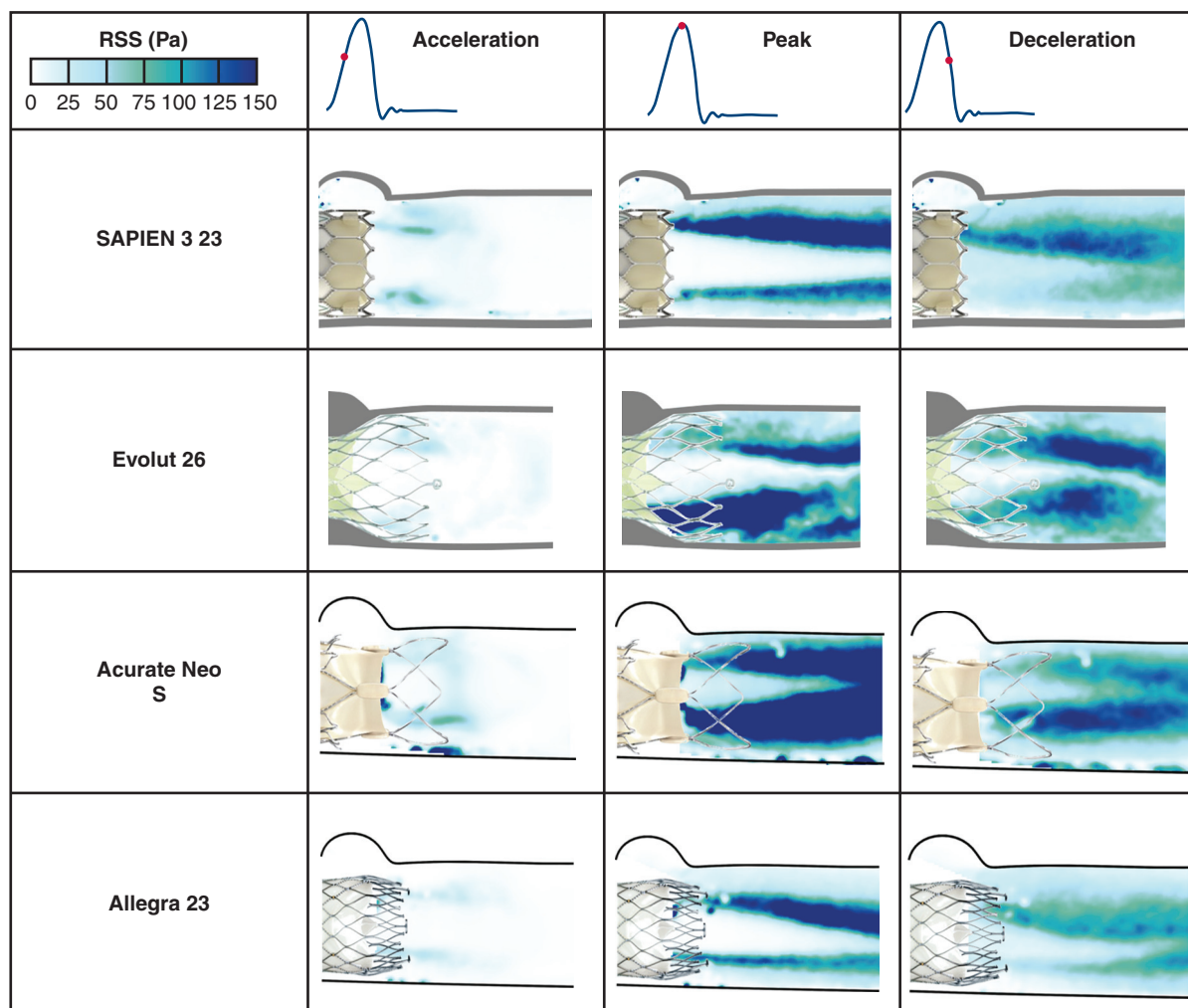


**FIGURE 2.** Principal Reynolds shear stresses (RSS) at different phases in the cardiac cycle. The dark blue patches indicate an elevated RSS magnitude, and the more prevalent elevated RSS magnitudes are, the more turbulent the flow is considered to be. Evolut R (Medtronic), Sapien 3 (Edwards Lifesciences), Acurate neo (Boston Scientific), and Allegra (New Valve Technologies).

the narrowest and where maximum jet velocity occurs). After that, the recovery process starts through a gradual increase in PG along the various points. All the valves follow this expected pattern of pressure changes along positions in the aortic root.

The largest pressure drop at the vena contracta occurs with the Acurate neo TAV where the minimal pressure reaches  $13.96 \pm 1.35$  mm Hg. The PG with the Sapien 3, Evolut, and Allegra reach  $10.54 \pm 0.51$  mm Hg,  $10.64 \pm 0.38$  mm Hg, and  $11.89 \pm 0.61$  mm Hg, respectively. The 23-mm Sapien 3 showed the smallest PG at the vena contracta. The location of the vena contracta varied with each valve. The vena contracta of the Acurate neo was the closest to the valve entrance, and that of the Allegra was the furthest from the valve entrance. At 12 mm, in the recovery zone, the smallest PG was obtained with the Allegra ( $3.32 \pm 0.94$  mm Hg), followed by Sapien 3 ( $3.68 \pm 0.76$  mm Hg), then the Evolut R

( $4.77 \pm 0.87$  mm Hg) and the largest PG was obtained with the Acurate neo ( $5 \pm 1.21$  mm Hg).

All differences in PGs were statistically significant ( $P < .001$ ) except for the Allegra and Sapien 3 at the vena contracta ( $P = .1399$ ) and the Acurate neo and Sapien 3 in recovery zone ( $P = .2105$ ).

The largest pressure recovery (difference between PG at the vena contracta and PG at 120 mm) was obtained with Acurate neo (8.96 mm Hg), followed by Allegra (7.79 mm Hg), then by Sapien 3 (6.86 mm Hg), and then Evolut R (4.47 mm Hg). From Figure 5, the fluctuations in the SDs are higher with the self-expanding valves compared with the Sapien 3. All differences in pressure recovery were statistically significant ( $P < .001$ ).

**DISCUSSION**

In this study, we evaluated the hemodynamics downstream of 4 TAVs with variable leaflet position, 3 of which

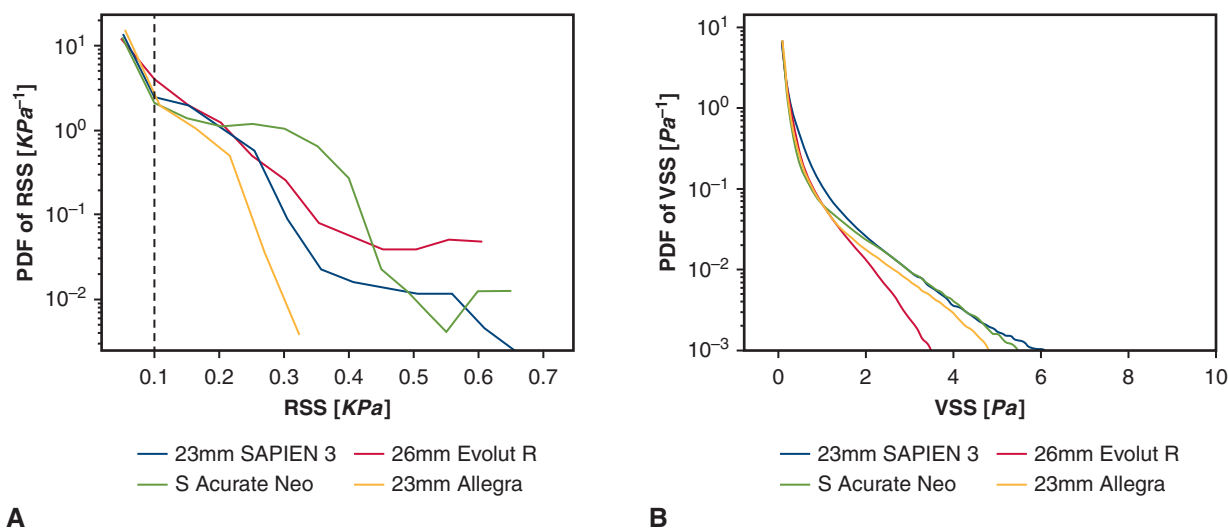


**FIGURE 3.** Probability density function (*PDF*) of the (A) Reynolds shear stress (*RSS*) distribution and the (B) viscous shear stress (*VSS*) distribution downstream of the Evolut R (Medtronic), Sapien 3 (Edwards Lifesciences), Acurate neo (Boston Scientific), and Allegra (New Valve Technologies) transcatheter aortic valves in semi-log scale. 0.1 KPa represents a potential blood damage threshold. The Acurate neo and the Evolut R present the largest distributions of *RSS* in all 3 phases (acceleration, peak systole, and deceleration). The Allegra shows the minimal range of *RSS* magnitudes (up to 320 Pa), followed by the Evolut R (up to 600 Pa) and then the Acurate neo and Sapien 3 (up to 650 Pa).

are self-expanding valves (26-mm Evolut R, S Acurate neo, and 23-mm Allegra) and 1 balloon expandable valve (23-mm Sapien 3). We report findings on flow turbulence and its relationship to potential for thrombogenicity due to flow turbulence, and on pressure recovery along with its relationship to the assessment of overall valve performance. The higher the *RSS* and the *VSS*, the more the flow is considered turbulent. Turbulence is an essential and important factor to assess after heart valve implantation because it can lead to blood damage such as platelet activation, thrombus formation, and hemolysis. Several studies have specified thresholds above which forces on the platelets are the red blood cells are nonphysiological, leading therefore to adverse effects related to blood damage.<sup>18,22</sup> Additionally, several clinical studies have pointed to the occurrence of thrombus formation and hemolysis after various generations of TAVs. These findings were dependent on the type of the valve implanted and how every unique valve design influences the resulting flow. Therefore, it is important to assess how valve performance and behavior (eg, gradients, turbulence, and flutter) influence or correlate with clinical findings.<sup>23-26</sup> The connection between blood damage and valve durability has also been a subject of research in the recent years.<sup>27,28</sup> Thus, understanding how every valve influences the resulting flow is important to relate the findings to future outcomes after TAV replacement.

In this study, the *RSS* (or turbulence shear stresses) were evaluated to compare the resulting turbulence obtained among the 4 valves. *RSS* is a pseudoforce and is often used to provide a statistical quantitative evaluation of the

influence of turbulent fluctuations on the averaged velocity field at a given position in space.<sup>18</sup> The Allegra TAV showed the smallest range of *RSS*, indicating lowest turbulence levels compared with the other valves. This result was also accompanied by a small leaflet flutter frequency (Videos 4 and 8), which helped with the flow stabilization and with the reduction of *RSS*.<sup>2</sup> The Acurate neo and the Evolut R showed elevated likelihoods of developing elevated *RSS* that exceed 0.1 KPa, a threshold adopted for blood damage initiation,<sup>21</sup> compared with the other valves. Both valves also showed elevated flutter frequency (Videos 1, 3, 5, and 7) influencing the elevated *RSS* obtained in this study. The elevated leaflet flutter could be attributed to the supra-annular design of the leaflets and the location of the tip of the leaflet in the Evolut R and the Acurate neo, in addition to the porcine pericardium material of the leaflets. Although this was clearly observed with these 2 self-expanding valves, the Allegra showed minimal flutter (comparable with the Sapien 3) despite having supra-annular leaflet design. This may be due to the small stent spaces (diamonds) and the compact frame of the Allegra compared with a more open stent design with both the Evolut R (larger diamonds) and the Acurate neo (open frame). This may also be due to tissue thickness and leaflet geometry that are most probably the main determinants of a complete circular opening and the degree of leaflet fluttering at the time of peak flow, which will ultimately determine flow patterns, turbulence, shear stresses, pressure drop, and pressure recovery.

Pressure recovery is an important phenomenon that instructs on the performance of the implanted valve.<sup>29</sup> As

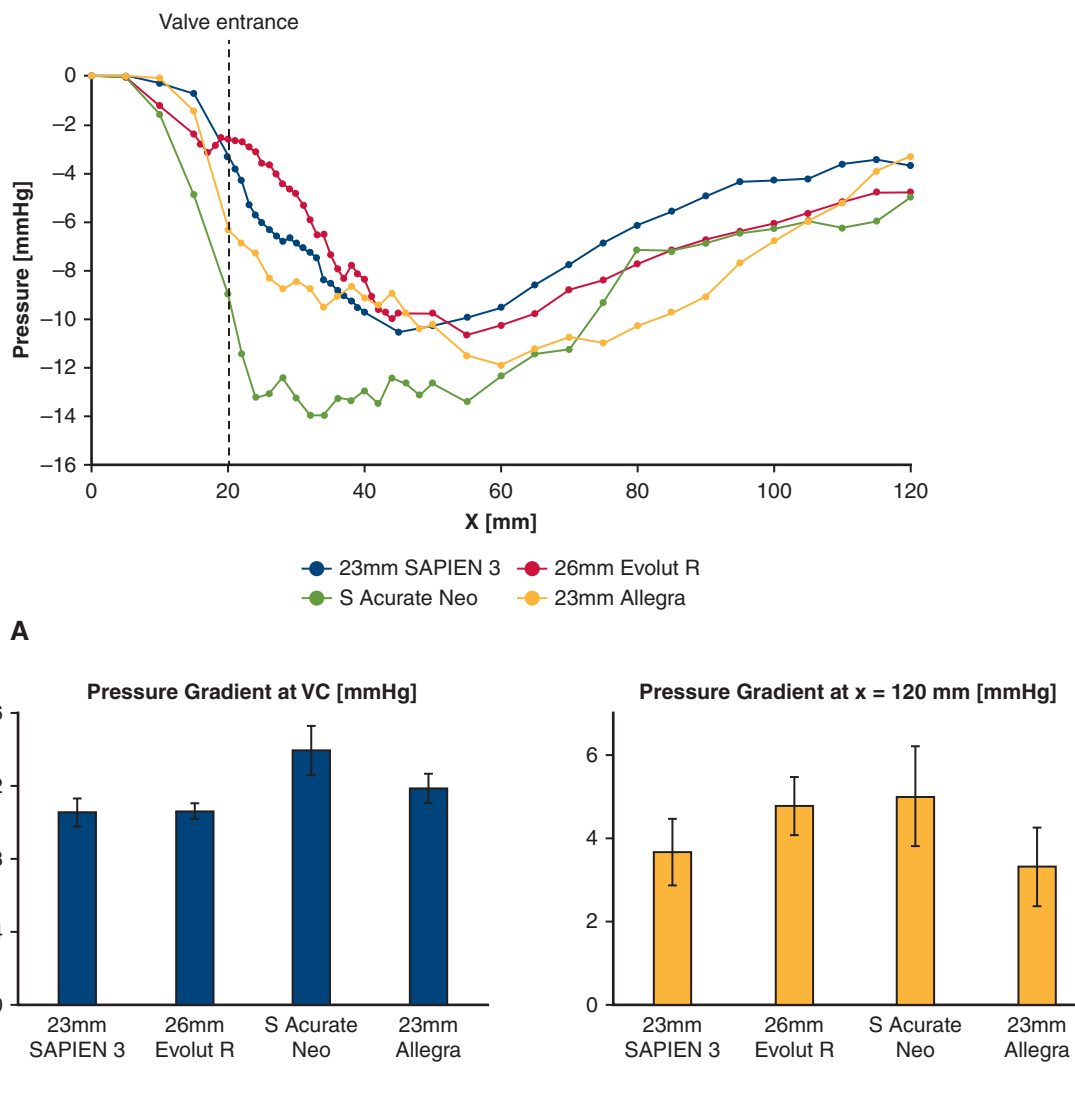


**FIGURE 4.** A, Variations of pressure gradients as a function of axial distance at selected location points during peak systole with the 23-mm Sapien 3 (Edwards Lifesciences), 26-mm Evolut R (Medtronic), S Acurate neo (Boston Scientific), and 23-mm Allegra (New Valve Technologies) transcatheter aortic valves. The results are plotted from the ventricular side upstream of each valve to the downstream side up until the end of the aortic testing chamber (at 120 mm). As the flow crosses the valve, the pressure gradient decreases from the ventricular side to the aortic one until it reaches a minimum at the vena contracta (VC) (where the jet is the narrowest and where maximum jet velocity occurs). After that, the recovery process starts through a gradual increase in pressure gradient along the various points. B, Bar plot showing the pressure gradients at the VC and the recovery zone at x = 120 mm. The dark lines on the bar plots indicate the SDs. The largest pressure drop at the VC occurs with the Acurate neo transcatheter aortic valve where the minimal pressure reaches  $13.96 \pm 1.35$  mm Hg. The pressure gradient with the Sapien 3, Evolut, and Allegra reach  $10.54 \pm 0.51$  mm Hg,  $10.64 \pm 0.38$  mm Hg, and  $11.89 \pm 0.61$  mm Hg, respectively. The 23-mm Sapien 3 showed the smallest pressure gradient at the VC. The location of the VC varied with each valve. The VC of the Acurate neo was the closest to the valve entrance, and that of the Allegra was the furthest from the valve entrance. At 12 mm, in the recovery zone, the smallest pressure gradient was obtained with the Allegra ( $3.32 \pm 0.94$  mm Hg), followed by Sapien 3 ( $3.68 \pm 0.76$  mm Hg), then the Evolut R ( $4.77 \pm 0.87$  mm Hg) and the largest pressure gradient was obtained with the Acurate neo ( $5 \pm 1.21$  mm Hg). All differences in pressure gradients were statistically significant ( $P < .001$ ) except for the Allegra and Sapien 3 at the VC ( $P = .1399$ ) and the Acurate neo and Sapien 3 in the recovery zone ( $P = .2105$ ).

the jet expands downstream, its velocity starts decreasing and pressure is recovered depending on several factors such as turbulence, velocity of blood at the vena contracta, and the geometry of the aorta.<sup>3,13,14,30</sup> Several clinical studies presented detailed comparative works

between echocardiogram-based gradients (at the vena contracta) and catheterization-based gradients (in the recovery zone).<sup>31-35</sup> Some of these studies highlighted that balloon-expandable valves are characterized by higher gradients at the vena contracta and more elevated



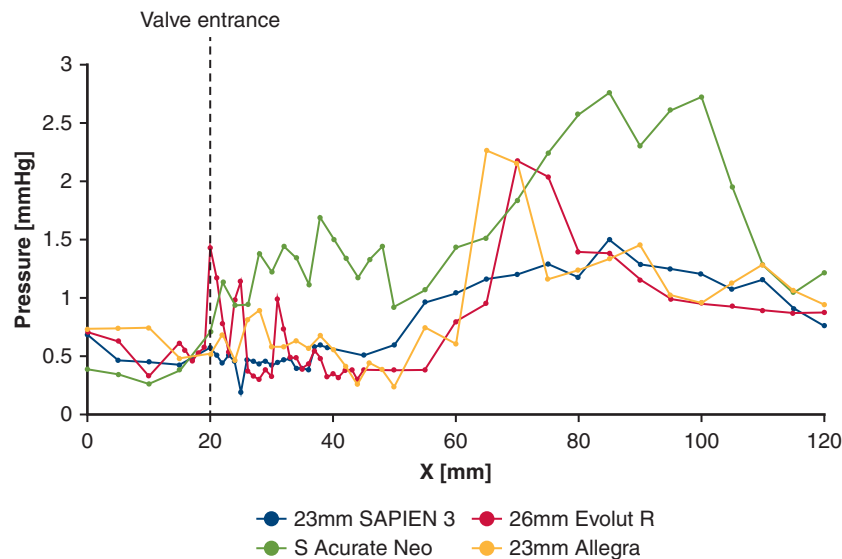


**FIGURE 5.** Variations of pressure gradient standard deviations as a function of axial distance at selected location points during peak systole with the 23-mm Sapien 3 (Edwards Lifesciences), 26-mm Evolut R (Medtronic), S Acurate neo (Boston Scientific), and 23-mm Allegra (New Valve Technologies) transcatheter aortic valves. The fluctuations in the standard deviations are higher with the self-expanding valves compared with the Sapien 3. This complements the elevated turbulent stresses obtained in this study.

pressure recovery.<sup>3,35</sup> Some of these studies were inconclusive.<sup>34</sup>

In this study, the Allegra TAV was characterized by the lowest PG in the recovery zone and one of the highest-pressure recoveries among the 4 valves. The Allegra, as previously mentioned, was characterized by the smallest turbulence downstream of the valve. The Acurate neo was characterized by elevated turbulence, the most elevated PG at the vena contracta and the most elevated PG at 120 mm. However, the pressure recovery obtained from the vena contracta to the 120-mm recovery zone was the highest. The turbulence downstream of the Evolut R was among the highest observed in this study, and the PG at the recovery zone was the second most elevated with the pressure recovery being the smallest. The effect of turbulence on the downstream flow of the valve was also clear with the large fluctuations in standard deviations of the PGs at the different locations. This study shows that pressure recovery is valve-dependent, although it is hard to generalize the dependence on the self-expanding versus the balloon-expandable type. With various valve types and designs, more experiments and more clinical outcomes are needed to assess the optimally performing valve type.

Although differences in gradients and pressure recovery among the four types of valves were demonstrated in this study, these differences may not be clinically significant in terms of hemodynamic performance. However, the opening and closing characteristics, the degree of fluttering and turbulence downstream the aorta may exert relevant influence in durability and long-term outcomes.

### Limitations

In this study, we used an idealized solid aortic root model that led to a perfect circular TAV replacement deployment, an advantage that may not be accomplished in many patients due to the anatomical characteristics of the native valve and root. The absence of patient-specific factors influence the flow patterns downstream of the valve and these characteristics have not been fully characterized at present in this study. However, we aimed at performing a highly controlled study that isolates the effect of each transcatheter heart valve independently from geometric or deployment-related considerations, similar to previous studies.<sup>9,36-40</sup> Moreover, in this study, only the recommended axial deployment<sup>41</sup> was assessed. Additionally, we performed the hemodynamic assessment of these valves under 1 physiological set of conditions. Whether or not these conclusions hold under different physiological scenarios is yet to be determined with more studies. Finally, we tested one type of valves for each experiment. Variability in valve type is not anticipated because the manufacturability of these commercial valves is already established. It is also key to acknowledge that such ex vivo modeling does not factor in the biological aspects of platelets activation which come into play.

### CONCLUSIONS

The hemodynamics downstream of 4 transcatheter aortic valves, 3 of which are self-expanding valves (26-mm Evolut R, S Acurate neo, and 23-mm Allegra) and 1 balloon expandable valve (23-mm Sapien 3) were evaluated in

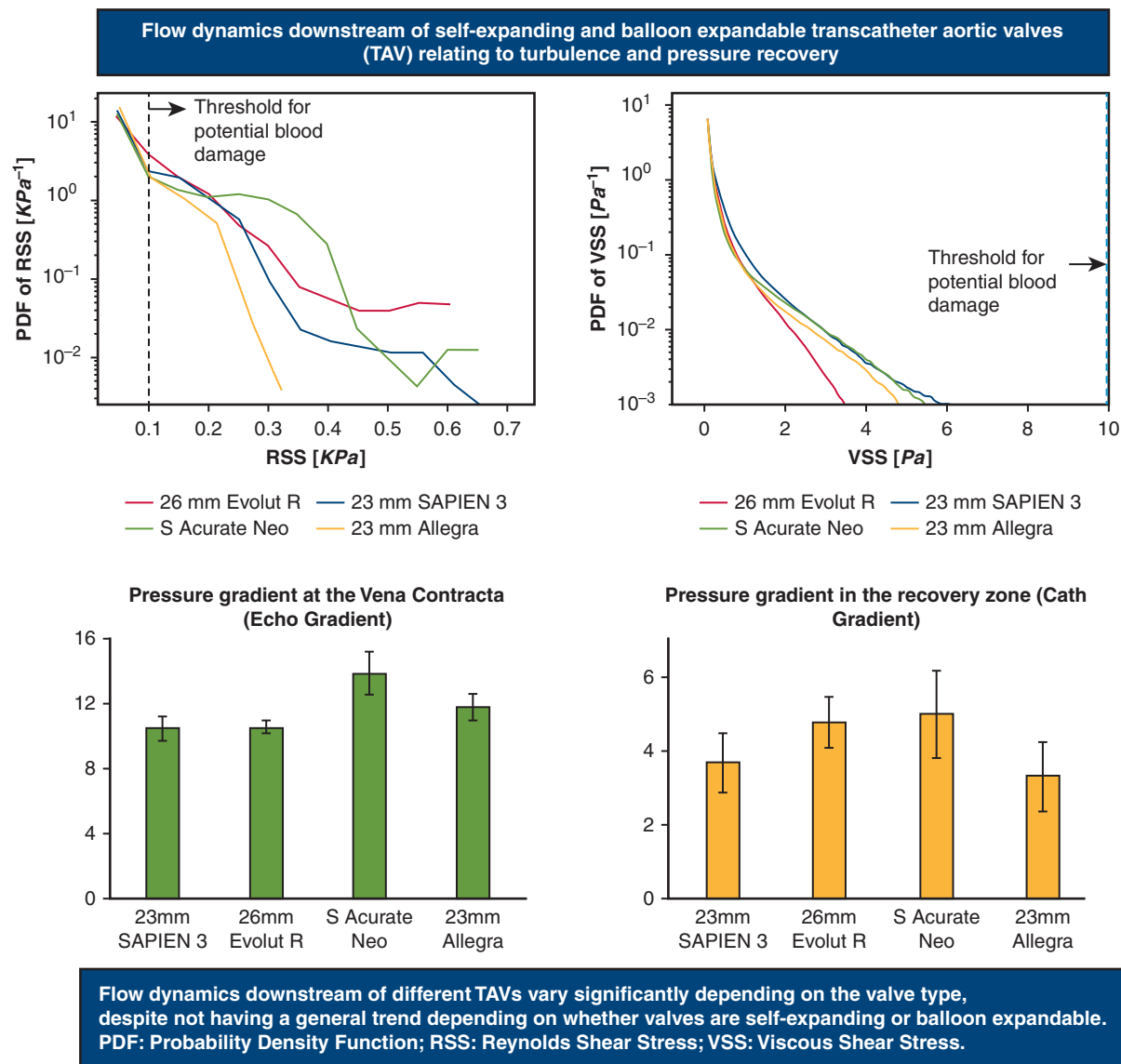


**FIGURE 6.** Flow dynamics downstream of self-expanding and balloon expandable transcatheter aortic valves (TAVs) relating to turbulence and pressure recovery. Evolut R (Medtronic), Sapien 3 (Edwards Lifesciences), Acurate neo (Boston Scientific), and Allegra (New Valve Technologies). *PDF*, Probability density function; *RSS*, Reynolds shear stress; *VSS*, viscous shear stress.

this study under pulsatile conditions in vitro. There was a distinct trend of performance obtained with each valve independent of whether they are self-expanding or balloon-expandable, as summarized in Figure 6. The Allegra valve, a self-expanding valve, and the Sapien 3 valve, a balloon-expandable valve, were characterized by the lowest leaflet flutter and thus, the lowest turbulence downstream. These results were supported by the lowest PG results along the pressure recovery zone and minimal fluctuations as evidenced by the SDs of the PG downstream of the valve.

**Conflict of Interest Statement**

Dr Hatoum has a patent application on predicting leaflet thrombosis modeling. Dr Dasi has patent applications filed

on novel polymeric valves, vortex generators, superhydrophobic/omniphobic surfaces, and predicting leaflet thrombosis modeling. Dr Thourani is a consultant for Abbott Vascular, Boston Scientific, Edwards Lifesciences, Cryo-life, Shockwave, and Jenavalve. Drs Hatoum, Thourani, and Dasi have filed patent application on computational predictive modeling of thrombosis in heart valves. Dr Sathanathan is a consultant to Edwards Lifesciences, Medtronic, Boston Scientific and NVT. Dr Kuetting is in the R&D department of New Valve Technology, the developer of the Allegra valve. All other authors reported no conflicts of interest.

The *Journal* policy requires editors and reviewers to disclose conflicts of interest and to decline handling or

reviewing manuscripts for which they have a conflict of interest. The editors and reviewers of this article have no conflicts of interest.

## References

- Bui HT, Khair N, Yeats B, Gooden S, James SP, Dasi LP. Transcatheter heart valves: a biomaterials perspective. *Adv Healthc Mater.* 2021;10:e2100115.
- Hatoum H, Yousefi A, Lilly S, Maureira P, Crestanello J, Dasi LP. An in vitro evaluation of turbulence after transcatheter aortic valve implantation. *J Thorac Cardiovasc Surg.* 2018;156:1837-48.
- Hatoum H, Hahn RT, Lilly S, Dasi LP. Differences in pressure recovery between balloon expandable and self-expandable transcatheter aortic valves. *Ann Biomed Engineer.* 2020;48:860-7.
- Abdel-Wahab M, Landt M, Neumann F-J, Massberg S, Frerker C, Kurz T, et al. 5-Year outcomes after TAVR with balloon-expandable versus self-expanding valves: results from the CHOICE randomized clinical trial. *Cardiovasc Intervent.* 2020;13:1071-82.
- Van Belle E, Vincent F, Labreuche J, Auffret V, Debry N, Lefèvre T, et al. Balloon-expandable versus self-expanding transcatheter aortic valve replacement: a propensity-matched comparison from the FRANCE-TAVI registry. *Circulation.* 2020;141:243-59.
- Hatoum H, Gooden S, Sathananthan J, Lilly S, Ihdahid AR, Thourani V, et al. Sinus and neo-sinus flow evaluation after implantation of an Evolut. Sapien 3, Acurate neo and Allegra transcatheter valves. *J Am Coll Cardiol.* 2021;77(18 Suppl 1):1708.
- González-García A, Hernandez H, Jurado-Román A, Galeote G, Santiago JV, Rodríguez L, et al. TCT-725 Comparative study of the hemodynamic performance of two latest generation supra-annular self-expanding transcatheter aortic valves (Allegra versus Acurate neo). *J Am Coll Cardiol.* 2019;74(13 Suppl): B711.
- Vahidkhan K, Azadani AN. Supra-annular valve-in-valve implantation reduces blood stasis on the transcatheter aortic valve leaflets. *J Biomechan.* 2017;58:114-22.
- Hatoum H, Dollery J, Lilly SM, Crestanello JA, Dasi LP. Implantation depth and rotational orientation effect on valve-in-valve hemodynamics and sinus flow. *Ann Thorac Surg.* 2018;106:70-8.
- Azadani AN, Reardon M, Simonato M, Aldea G, Nickenig G, Kornowski R, et al. Effect of transcatheter aortic valve size and position on valve-in-valve hemodynamics: an in vitro study. *J Thorac Cardiovasc Surg.* 2017;153:1303-15.e1.
- Simonato M, Webb J, Kornowski R, Vahanian A, Frerker C, Nissen H, et al. Transcatheter replacement of failed bioprosthetic valves: large multicenter assessment of the effect of implantation depth on hemodynamics after aortic valve-in-valve. *Circ Cardiovasc Interv.* 2016;9:e003651.
- Hatoum H, Dollery J, Lilly SM, Crestanello J, Dasi LP. Impact of patient-specific morphologies on sinus flow stasis in transcatheter aortic valve replacement: an in vitro study. *J Thorac Cardiovasc Surg.* 2019;157:540-9.
- Samae M, Hatoum H, Thourani V, Yoganathan A, Dasi LP. Effect of ascending aorta size in transcatheter aortic valve performance: comparison between Evolut R and Sapien 3. *J Am Coll Cardiol.* 2021;77(18 Suppl 1):1768.
- Samae M, Hatoum H, Biersmith M, Yeats B, Gooden SC, Thourani VH, et al. Gradient and pressure recovery of a self-expandable transcatheter aortic valve depends on ascending aorta size: in vitro study. *J Thorac Cardiovasc Surg Open.* 2022;9:28-38.
- Herrmann HC, Laskey WK. Pressure loss recovery in aortic valve stenosis: contemporary relevance. *Catheter Cardiovasc Interv.* 2022;99:195-7.
- Jones SA. A relationship between Reynolds stresses and viscous dissipation: implications to red cell damage. *Ann Biomed Engineer.* 1995;23:21-8.
- Hatoum H, Moore BL, Maureira P, Dollery J, Crestanello JA, Dasi LP. Aortic sinus flow stasis likely in valve-in-valve transcatheter aortic valve implantation. *J Thorac Cardiovasc Surg.* 2017;154:32-43.e1.
- Ge L, Dasi LP, Sotiropoulos F, Yoganathan AP. Characterization of hemodynamic forces induced by mechanical heart valves: Reynolds vs. viscous stresses. *Ann Biomed Engineer.* 2008;36:276-97.
- Hatoum H, Maureira P, Dasi LP. A turbulence in vitro assessment of On-X and St Jude Medical prostheses. *J Thorac Cardiovasc Surg.* 2020;159:88-97.
- Hatoum H, Askegaard G, Iyer R, Prasad Dasi L. Atrial and ventricular flows across a transcatheter mitral valve. *Interac Cardiovasc Thorac Surg.* 2021;33:1-9.
- Dasi LP, Simon HA, Sucusky P, Yoganathan AP. Fluid mechanics of artificial heart valves. *Clin Exper Pharmacol Physiol.* 2009;36:225-37.
- Sotiropoulos F, Le TB, Gilmanov A. Fluid mechanics of heart valves and their replacements. *Annu Rev Fluid Mech.* 2016;48:259-83.
- Chakravarty T, Søndergaard L, Friedman J, De Backer O, Berman D, Kofoed KF, et al. Subclinical leaflet thrombosis in surgical and transcatheter bioprosthetic aortic valves: an observational study. *Lancet.* 2017;389:2383-92.
- Yanagisawa R, Tanaka M, Yashima F, Arai T, Jinzaki M, Shimizu H, et al. Early and late leaflet thrombosis after transcatheter aortic valve replacement: a multicenter initiative from the OCEAN-TAVI Registry. *Circ Cardiovasc Interv.* 2019;12:e007349.
- Svensson LG, Blackstone EH, Rajeswaran J, Brozzi N, Leon MB, Smith CR, et al. Comprehensive analysis of mortality among patients undergoing TAVR: results of the PARTNER trial. *J Am Coll Cardiol.* 2014;64:158-68.
- Eleid MF, Cabalka AK, Malouf JF, Sanon S, Hagler DJ, Rihal CS. Techniques and outcomes for the treatment of paravalvular leak. *Circ Cardiovasc Interv.* 2015;8:e001945.
- Egbe AC, Pislaru SV, Pellikka PA, Poterucha JT, Schaff HV, Maleszewski JJ, et al. Bioprosthetic valve thrombosis versus structural failure: clinical and echocardiographic predictors. *J Am Coll Cardiol.* 2015;66:2285-94.
- Sellers SL, Turner CT, Sathananthan J, Cartledge TR, Sin F, Bouchareb R, et al. Transcatheter aortic heart valves: histological analysis providing insight to leaflet thickening and structural valve degeneration. *JACC Cardiovasc Imaging.* 2019;12:135-45.
- Bahlmann E, Cramariuc D, Gerds E, Gohlke-Baerwolf C, Nienaber CA, Eriksen E, et al. Impact of pressure recovery on echocardiographic assessment of asymptomatic aortic stenosis: a SEAS substudy. *JACC Cardiovasc Imaging.* 2010;3:555-62.
- Bach DS. Echo/Doppler evaluation of hemodynamics after aortic valve replacement: principles of interrogation and evaluation of high gradients. *JACC Cardiovasc Imaging.* 2010;3:296-304.
- Abbas AE, Mando R, Hanzel G, Gallagher M, Safian R, Hanson I, et al. Invasive versus echocardiographic evaluation of transvalvular gradients immediately post-transcatheter aortic valve replacement: demonstration of significant echocardiography-catheterization discordance. *Circ Cardiovasc Interv.* 2019;12:e007973.
- Baumgartner H, Khan S, Derobertis M, Czer L, Maurer G. Discrepancies between Doppler and catheter gradients in aortic prosthetic valves in vitro. A manifestation of localized gradients and pressure recovery. *Circulation.* 1990;82:1467-75.
- Alston MM, Nader Hatoum H, Yeats B, Egbuche O, Biswas M, Orsinelli D, et al. Comparison of catheterization versus echocardiographic based gradients in balloon expandable versus self expanding transcatheter aortic valve implantation. *J Invasive Cardiol.* Forthcoming 2022.
- Mando R, Elmariah S, Hanzel G, Camacho A, Selberg A, Al-Azizi K, et al. TCT CONNECT-91 invasive versus echocardiographic gradients post valve-in-valve TAVR: a multicenter trial. *J Am Coll Cardiol.* 2020;76:B40-1.
- Bavry AA, Aalaei-Andabili SH, Okuno T, Kumbhani DJ, Stortecky S, Asami M, et al. Transvalvular gradients for balloon-expandable and self-expanding valves. *J Invasive Cardiol.* 2020;32:E258-60.
- Hatoum H, Lilly S, Maureira P, Crestanello J, Dasi LP. The hemodynamics of transcatheter aortic valves in transcatheter aortic valves. *J Thorac Cardiovasc Surg.* 2021;161:565-76.
- Hatoum H, Dasi LP. Spatiotemporal complexity of the aortic sinus vortex as a function of leaflet calcification. *Ann Biomed Engineer.* 2019;47:1116-28.
- Hatoum H, Maureira P, Lilly S, Dasi LP. Impact of leaflet laceration on transcatheter aortic valve-in-valve washout: BASILICA to solve neosinus and sinus stasis. *JACC Cardiovasc Interv.* 2019;12:1229-37.
- Hatoum H, Maureira P, Lilly S, Dasi LP. Impact of BASILICA on sinus and neosinus hemodynamics after valve-in-valve with and without coronary flow. *Cardiovasc Revasculariz Med.* 2020;21:271-6.
- Hatoum H, Maureira P, Lilly S, Dasi LP. Leaflet laceration to improve neosinus and sinus flow after valve-in-valve. *Circ Cardiovasc Interv.* 2019;12:e007739.
- Bapat V. Valve-in-valve apps: why and how they were developed and how to use them. *EuroIntervention.* 2014;10:U44-51.

**Key Words:** TAVR, turbulence, blood damage, pressure recovery

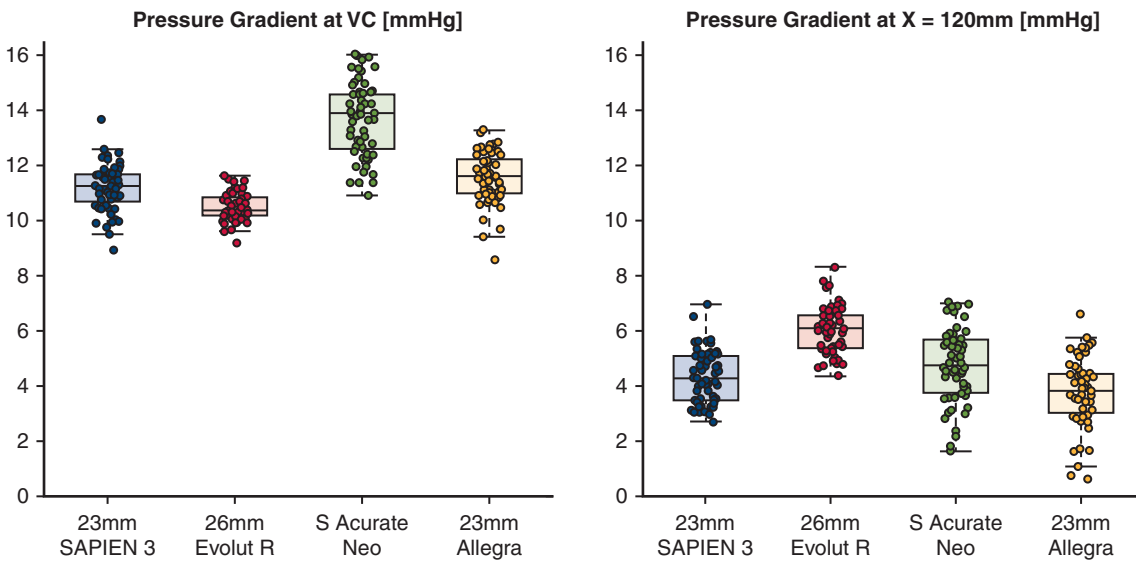


**FIGURE E1.** Box-and-whisker plot showing the pressure gradient distribution for each valve case. The lower and upper borders of the box ( $Q_1$  and  $Q_3$ ) represent the lower and upper quartiles (25th percentile and 75th percentile). The middle horizontal line ( $Q_2$ ) represents the middle value in the data set (50th percentile). The lower and upper lines ( $Q_0$  and  $Q_4$ , which are known as whiskers) represent variability outside the upper and lower quartiles (0th percentile and 100th percentile, respectively) and show the minimum and maximum values of nonoutliers. Extra dots represent outliers, which differ significantly from the rest of the dataset. Evolut R (Medtronic), Sapien 3 (Edwards Lifesciences), Acurate neo (Boston Scientific), and Allegra (New Valve Technologies). VC, Vena contracta.